HHS Public Access

Author manuscript

Arterioscler Thromb Vasc Biol. Author manuscript; available in PMC 2016 October 01.

Published in final edited form as:

Arterioscler Thromb Vasc Biol. 2015 October ; 35(10): 2092–2103. doi:10.1161/ATVBAHA.115.305843.

Monocyte-derived dendritic cells upregulate extracellular catabolism of aggregated LDL upon maturation, leading to foam cell formation

Abigail S. Haka[1], **Rajesh K. Singh**[1], **Inna Grosheva**[1], **Haley Hoffner**[1], **Estibaliz Capetillo-Zarate**[1,3], **Harvey F. Chin**[1], **Niroshana Anandasabapathy**[2], and **Frederick R. Maxfield**[1]

[1]Department of Biochemistry, Weill Cornell Medical College, New York, NY 10065, USA

[2]Department of Dermatology, Harvard Skin Disease Research Center, Bringham and Women's Hospital, Boston, MA 02115, USA

Abstract

Objective—Although dendritic cells are known to play a role in atherosclerosis, few studies have examined the contribution of the wide variety of dendritic cell subsets. Accordingly, their roles in atherogenesis remain largely unknown. We investigated the ability of different dendritic cell subsets to become foam cells following contact with aggregated LDL (the predominant form of LDL found in atherosclerotic plaques).

Approach and Results—We demonstrate that both murine and human monocyte-derived dendritic cells use exophagy to degrade aggregated LDL, leading to foam cell formation, while monocyte-independent dendritic cells are unable to clear LDL aggregates by this mechanism. Exophagy is a catabolic process in which objects that cannot be internalized by phagocytosis (due to their size or association with extracellular structures) are initially digested in an extracellular acidic lytic compartment. Surprisingly, we found that monocyte-derived dendritic cells upregulate exophagy upon maturation. This contrasts various forms of endocytic internalization in dendritic cells, which decrease upon maturation. Finally, we show that our *in vitro* results are consistent with dendritic cell lipid accumulation in plaques of an $ApoE^{-/-}$ mouse model of atherosclerosis.

Conclusions—Our results show that monocyte-derived dendritic cells use exophagy to degrade aggregated LDL and become foam cells, while monocyte-independent dendritic cells are unable to clear LDL deposits. Further, we find that exophagy is upregulated upon dendritic cell maturation. Thus, exophagy-mediated foam cell formation in monocyte-derived dendritic cells could play a significant role in atherogenesis.

Keywords

dendritic cell; exophagy; aggregated LDL; foam cell

Corresponding Author: Frederick R. Maxfield, Department of Biochemistry, Box 63, Weill Cornell Medical College, 1300 York Avenue, New York, NY 10065, frmaxfie@med.cornell.edu, Tel: 212 746 6405, Fax: 212 746 8875.

[3]Current affiliation: IKERBASQUE, Basque Foundation for Science, 48011, Bilbao, Spain; Achucarro Basque Center for Neurosciences, 48170, Zamudio, Spain; Department of Neuroscience, Faculty of Medicine and Odontology, University of the Basque Country EHU/UPV, Leioa, Spain.

Disclosures: None

Introduction

Atherosclerosis is a lipid-related inflammatory disease in which the interaction of immune cells with subendothelial lipoproteins and ensuing foam cell formation play a pivotal role. While macrophages are the predominant immune cells associated with atherosclerosis, almost 20 years ago, Bobryshev and Lord used electron microscopy to demonstrate that dendritic cells (DCs) are also present in human arteries[1–3]. Since then, several studies have shown the accumulation of DCs in human and murine atherosclerotic lesions using a variety of markers[4–14]. In addition to regulation of the inflammatory response[11, 15, 16], DCs also play a direct role in the regulation and processing of lipid[17, 18]. Conditional depletion of $CD11c^+$ cells in low-density lipoprotein receptor knockout (Ldlr−/−) mice, significantly reduced the intimal lipid area, and few foam cells were found, suggesting that DCs may be responsible for foam cell formation at the earliest stages of plaque development[18]. Although this study indicated a pro-atherogenic role for dendritic cells, it did not differentiate between the wide variety of dendritic cell subsets, and accordingly their roles in atherogenesis remain largely unknown.

Both classical DCs, formed by the cytokine fms-like tyrosine kinase 3 ligand (flt-3) acting on monocyte-independent precursors[19–21], and non-classical (monocyte-derived) DCs[22] are present in atherosclerotic plaques[11]. Recently, the Steinman laboratory examined the role of classical flt-3 derived DCs in atherosclerosis and, surprisingly, found that they appear to be atheroprotective[11]. Other studies have used various manipulations to perturb non-classical monocyte-derived DC function in mouse models of atherosclerosis, such as restricted monocyte entry using CX3CR1-deficient mice[23] or inhibited monocyte differentiation into DCs using granulocyte macrophage colony-stimulating factor (GM-CSF) deficient mice[24, 25]. While atherosclerosis was decreased when monocyte plaque entry was restricted, suggesting a pro-atherogenic role for non-classical monocyte-derived DCs, loss of CX3CR1 concomitantly reduces macrophage plaque accumulation[26], leaving the relative contribution of these two cell types to atherogenesis unresolved. Further, studies using GM-CSF deficient mice report conflicting phenotypes, so the role of non-classical monocyte-derived DCs in atherosclerosis remains elusive.

In the arterial intima, lipid accumulation can be found within vascular $CD11c^+$ DCs in Ldlr −/− mice after only a few days of hypercholesterolemia, where they adopt a foam cell-like appearance that may constitute the earliest stages of plaque formation[18]. Historically, the macrophage has been the predominant lesional cell type studied to assess foam cell formation during atherogenesis. While, macrophage foam cell formation is generally considered atherogenic[27], there are several notable differences between macrophages and DCs that are relevant for the biological consequences of lipid loading. For instance, molecules involved in handling cholesterol, such as ATP-binding cassette (ABC) A1 and ABCG1 are differentially expressed by macrophages and DCs (http://www.immgen.org). Also, macrophage migration and ensuing emigration from tissues is much less efficient than that of DCs[28], although evidence suggests that hypercholesterolemia affects DC mobilization[29]. Thus, it is possible that the consequences of foam cell formation by these two cell types may be quite disparate. While macrophage foam cell formation has received

much attention, the mechanism(s) by which DCs internalize lipoproteins to become foam cells and the functional significance of DC lipid accumulation remains to be determined.

In atherosclerotic plaques, more than 90% of the low density lipoprotein (LDL) that immune cells interact with is aggregated and avidly bound to the subendothelial matrix[30–32]. This aggregated LDL (agLDL) can be modified by oxidation and exposure to lipases. Mouse models in which the subendothelial retention of LDL is blocked develop significantly less atherosclerosis than their wild type counterparts, with lesion area reduced by as much as 86%[33]. Thus, mechanisms of foam cell formation based on catabolism of agLDL likely have significant physiological relevance. However, most studies of foam cell formation employ modified monomeric LDL, such as oxidized, acetylated or minimally modified LDL[34, 35]. The contributions of these different pathways to foam cell formation in atherosclerosis are not known. In a cell culture model of the interaction of macrophages with agLDL, we showed that the macrophages create deeply invaginated structures that are actively acidified in which extracellular agLDL is digested by exocytosed lysosomal enzymes[36]. We describe this method of catabolism as exophagy and the compartment used for degradation as a lysosomal synapse.

In light of research indicating that DCs play an important role in atherosclerotic lesion development, we investigated the ability of both moncyte-independent (flt-3 derived, classical) and monocyte-derived (GM-CSF derived, non-classical) DCs to perform exophagy-mediated catabolism of agLDL. We found that, similar to macrophages (which also derive from monocytes), GM-CSF bone marrow-derived DCs use exophagy to degrade agLDL and that this interaction leads to foam cell formation. Conversely, flt-3 bone marrow-derived DCs did not perform exophagy, did not become foam cells and were unable to degrade the aggregate. Next, we compared the ability of immature and mature monocyte-derived DCs to perform exophagy as it is well known that several types of endocytosis are dampened during non-classical DC maturation[37, 38]. Surprisingly, we found that mature DCs (mDC) upregulate exophagy and consequently, take up more cholesterol from the aggregates than immature DCs (iDC). Finally, we show that consistent with our *in vitro* cell culture results, mDC contain more neutral lipid than iDC in an $ApoE^{-/-}$ mouse model of atherosclerosis, while monocyte-independent DC contained scant amounts of lipid. These results show that monocyte-derived DCs can use exophagy to degrade agLDL that is not taken up by standard phagocytic mechanisms and that in contrast to other forms of endocytosis, exophagy is upregulated upon DC maturation. We suggest that exophagy-mediated foam cell formation in monocyte-derived DCs could play a significant role in atherogenesis.

Materials and Methods

Materials and Methods are available in the online-only Data Supplement.

Results

GM-CSF bone marrow-derived DCs form specialized extracellular compartments at sites of contact with agLDL

To characterize the topological organization of compartments formed for exophagy, we labeled the plasma membrane with fluorescent cholera toxin B (CtB)[36, 39]. In this experiment the cells are not permeabilized, so the macromolecular CtB can only label glycolipids on the plasma membrane. We use this technique to examine whether plasma membrane surrounds the aggregate, thereby establishing the surface connectivity of the compartment. We note lipid molecules and even GPI-anchored proteins can redistribute on the plasma membrane following fixation with 3% paraformaldehyde (PFA)[40], so we would expect the G_{M1} ganglioside, which binds CtB, to remain mobile after fixation. Both flt-3 bone marrow-derived and GM-CSF bone marrow-derived primary murine DCs were incubated with AlexaFluor-546 (Alexa546)-agLDL for 60 min, labeled with Alexa488-CtB on ice for 3 min and fixed. Sites of contact between GM-CSF bone marrow-derived DCs and agLDL were labeled by CtB (arrows, Figure 1A and B), indicating that the aggregate is contained in a compartment that is connected to the cell surface. An axial slice through the confocal stack at the position of the red line shows that, although the aggregate resembles a separate vesicle in the xy plane (Figure 1B), it is contained in a compartment contiguous with the extracellular space (Figure 1B′). In contrast, flt-3 bone marrow-derived DCs do not create deeply invaginated structures at sites of contact with the aggregate (arrows, Figure 1C and D), indicating that they do not form specialized extracellular compartments in response to contact with agLDL. We note that the flt-3 bone marrow-derived DC culture contains a mix of two distinct $CD24^{high}$ and $CD11b^{high}$ DCs, equivalent to splenic CD8+ and CD8− DCs, as well as $CD45RA^{high}$ plasmacytoid DCs[41]. Sufficient agLDL was added to the culture system so that >95% of cells were in contact with aggregate. None of the cells in our mixed flt-3 bone marrow-derived DC culture formed extracellular compartment in response to contact with agLDL, indicating that both types of flt-3 bone marrow-derived DCs were unresponsive to the agLDL.

Compartments used for exophagy are formed via F-actin driven membrane protrusions surrounding the aggregate[39]. We examined F-actin near sites of contact with agLDL in both flt-3 bone marrow-derived and GM-CSF bone marrow-derived primary murine DCs. Cells were incubated with Alexa546-agLDL followed by fixation and labeling of F-actin by Alexa488-phalloidin (Figure 1 E–H). After a 60 min agLDL incubation, an enrichment of F-actin was detected near the sites of contact with agLDL in GM-CSF bone marrow-derived (arrows, Figure 1E and F) but not appreciably in flt-3 bone marrow-derived DCs (Figure 1G and H). Again, no cells in our mixed flt-3 bone marrow-derived DC culture formed local F-actin structures in response to contact with agLDL. We also examined primary flt-3 derived DCs isolated from spleens of mice treated with flt-3 ligand. Supplemental Figure I shows roughly a 20-fold expansion of splenic flt-3 derived DCs upon treatment with flt-3 ligand. No increase in local F-actin was seen at points of contact between primary flt-3 derived DCs and agLDL (data not shown). Actin polymerization, typical of a lysosomal synapse, was confirmed in human monocyte-derived DCs (huMDDCs). Local F-actin rich structures were detected near the sites of contact with agLDL in huMDDCs (arrows, Figure 1I and J). Both

the local F-actin rich structures and CtB staining indicate that GM-CSF bone marrow-derived DCs form deeply invaginated surface compartments in response to incubation with agLDL but flt-3 bone marrow-derived DCs do not.

GM-CSF bone marrow-derived DCs form a lysosomal synapse to degrade agLDL but flt-3 bone marrow-derived DCs are unable to clear agLDL

We have previously reported that compartments used for extracellular catabolism, described as a lysosomal synapse, function as an extracellular hydrolytic organelle due to targeted exocytosis of lysosomes and compartment acidification by V-ATPase on the plasma membrane[36]. We tested whether lysosomal contents, which include lysosomal acid lipase (LAL), a lysosomal hydrolase essential for the intracellular degradation of cholesteryl esters, were delivered to points of contact with the aggregate in both flt-3 and GM-CSF bone marrow-derived DCs. Biotin-fluorescein-dextran was incubated with DCs overnight, leading to endocytosis of the dextran and delivery to lysosomes[42]. Cells were then exposed to streptavidin-Alexa546-labeled agLDL for 90 min followed by a 30 sec treatment with biotin-Alexa633 to label extracellular aggregates. Next, excess biotin was applied to block any remaining free streptavidin on the aggregates. Cells were then fixed and permeabilized to remove the bright lysosomal fluorescence and facilitate identification of the exocytosed fluorescein signal.

When GM-CSF bone marrow-derived DCs were in contact with agLDL for 90 min (Figure 2A–D) there was significant deposition of biotin-fluorescein-dextran onto the aggregate in regions in contact with cells (arrows, Figure 2A). Consistent with previous studies, the biotin-Alexa633 staining (Figure 2D) clearly indicated that the aggregate was largely extracellular after the 90 min incubation[43]. We have previously shown that the extracellular compartments formed by macrophages are dynamic, allowing catabolic products and lysosomal enzymes to be released into the extracellular space as well as the entry of large molecules, such as biotinylated fluorophores[36]. While we display a compartment that is positive for Alexa633, we note that many regions of exocytosis excluded biotin-Alexa633 (data not shown). Co-localization of the fluorescein and Alexa633 signals demonstrated that lysosomal contents were exocytosed and delivered to an extracellular compartment in GM-CSF bone marrow-derived DCs. Consistent with our findings regarding compartment formation, no lysosomal exocytosis was seen at points of contact between the aggregate and any of the flt-3 bone marrow-derived DCs in the mixed culture (Figure 2E–G). We also observed no lysosome exocytosis in primary flt-3 derived DCs isolated from mouse spleen (data not shown). Lysosome exocytosis to an extracellular agLDL-containing compartment was also seen in huMDDCs (arrows, Figure 2H–J). These data show that lysosomal contents were delivered to an extracellular compartment, and the previously internalized biotin-fluorescein-dextran became associated with the agLDL contained in these compartments in GM-CSF bone marrow-derived but not flt-3 bone marrow-derived DCs.

Finally, we tested whether portions of extracellular compartments formed at points of contact with the aggregate were acidified in flt-3 and GM-CSF bone marrow-derived DCs. In order for LAL or other secreted lysosomal acid hydrolases to function optimally, an acidic environment is required. To test whether portions of the compartment are acidified,

we labeled LDL with CypHer 5E, a pH sensitive fluorophore, and Alexa488, a pH insensitive fluorophore[44]. DCs were incubated with agLDL, and the pH surrounding the aggregate was determined from the ratio of CypHer 5E to Alexa488 fluorescence as compared to values obtained in pH calibration buffers. When GM-CSF bone marrow-derived DCs interacted with the dual labeled agLDL, regions of low pH could be seen at the contact sites (arrow, Figure 2K). Consistent with our data regarding compartment formation and lysosome exocytosis, no acidification was observed in aggregates in contact with any flt-3 bone marrow-derived DCs in the mixed culture (Figure 2L). Regions of low pH were also seen in contact sites between huMDDCs and agLDL (arrow, Figure 2M).

To determine whether cholesteryl ester hydrolysis occurs in extracellular compartments formed for exophagy, we used filipin, a fluorescent sterol-binding polyene that can be used for detection of free cholesterol[45]. Flt-3 and GM-CSF bone marrow-derived DCs were incubated with Alexa546-agLDL for 1 hr, fixed and labeled with filipin (Figure 2N and O). As expected, GM-CSF bone marrow-derived DCs exhibited intense filipin staining (green) in the region of contact with the agLDL (arrows, Figure 2N), while flt-3 bone marrow-derived DCs did not exhibit filipin staining near the aggregate (Figure 2O). The bright filipin labeling seen in GM-CSF bone marrow-derived DCs indicates there is an increase in free cholesterol at sites of contact between agLDL and the cell.

GM-CSF bone marrow-derived DCs use exophagy to degrade agLDL and become foam cells

Next, we investigated whether incubation of flt-3 and GM-CSF bone marrow-derived DCs with agLDL leads to exophagy-mediated foam cell formation. Flt-3 and GM-CSF bone marrow-derived DCs were incubated with Alexa546-agLDL for 0, 2, 4, 6 and 24 hours. At each time point the cells were fixed and labeled with LipidTOX-Green to detect neutral lipid droplets, indicative of foam cell formation (arrows, Figure 3A and B). The percentage of LipidTOX-positive cells was quantified for each time point. Consistent with previous results, we did not observe foam cell formation when flt-3 bone marrow-derived DCs were incubated with agLDL (Figure 3C–E). The number of GM-CSF bone marrow-derived DCs in contact with aggregates that were LipidTOX-positive increased as a function of agLDL incubation time indicating increased levels of intracellular neutral lipid (Figure 3E). This shows that *in vitro*, GM-CSF bone marrow-derived DCs use exophagy to degrade agLDL and become foam cells.

Foam cell formation is accompanied by increases in cellular free cholesterol. To assess the effects of increasing cellular cholesterol on exophagy, we raised cellular free cholesterol levels and examined local actin polymerization and lysosome exocytosis to the compartment. To increase cellular free cholesterol, GM-CSF bone marrow-derived DC were treated with 5mM cholesterol:methyl-β-cyclodextrin (MβCD) for 15 min. Treated and resting DC were then incubated with agLDL in the presence of an acyl-coenzyme A cholesterol acyltransferase (ACAT) inhibitor to maintain cellular free cholesterol levels (*i.e.*, prevent esterification of cholesterol) for the duration of the experiment. Under the conditions used in these experiments, the cellular free cholesterol level in treated cells was increased 1.7-fold over resting cells as determined by analysis of cellular lipid extracts using gas

chromatography-mass spectrometry (GC-MS). The cellular free cholesterol was visualized using filipin staining, which revealed an increase in free cholesterol in cholesterol-MβCD treated DCs (Figure 3F and G) compared to resting DCs (Figure 3H and I). Both compartment formation, quantified by local F-actin rich structures (Figure 3J), and lysosome exocytosis (Figure 3K) were unaffected by a substantial increase in cellular free cholesterol levels.

DC maturation results in an upregulation of exophagy

It is well established that down regulation of endocytosis, including macropinocytosis, phagocytosis and efferocytosis, occurs with DC maturation[37, 38]. Thus, we wondered if exophagy would also be down regulated upon DC maturation. To this end, the ability of GM-CSF bone marrow-derived iDCs and mDCs to form a lysosomal synapse and perform exophagy-mediated catabolism of agLDL was compared. mDCs were generated on day 10 of GM-CSF culture by overnight treatment with LPS and examined on day 11. First, the formation of F-actin in iDCs and mDCs near sites of contact with agLDL was examined. Both iDCs and mDCs were incubated with Alexa546-agLDL for 60 min followed by fixation and labeling of F-actin with Alexa488-phalloidin. After 60 min, an enrichment of F-actin was detected near the sites of contact with agLDL in both iDCs (Figure 4A and B) and mDCs (Figure 4C and D). Surprisingly, the local F-actin in mDCs was significantly more intense than that observed in iDCs. The iDC culture represents a mixed population of cells[46]. The main contaminants are macrophages and B cells. However, macrophages adhere strongly to the culture dish and are not resuspended with the DCs when they are plated for experiments, while B cells are non-adherent and do not stick to our microscopy dishes. Zbtb46 classical DCs are a minor contaminant in this culture system but are also non-adherent. To ensure that contaminant cells were not affecting our F-actin measurements, we isolated $CD11c^+$ cells from the culture using flow cytometry. No quantitative difference was seen in the amount of local F-actin polymerization between the unsorted culture and the isolated $CD11c^+$ iDC cells (Supplemental Figure IIA), indicating that the cells used for microscopy experiments represent a homogenous population of $CD11c^+$ iDC.

Quantification of the average local F-actin intensity per cell revealed a 60% increase in mature murine DCs compared to immature murine DCs (Figure 4E). Further, we examined the formation of the lysosomal synapse in immature and mature huMDDCs and found a similar increase in local F-actin rich structures used for compartment formation in mDCs compared to iDCs (Figure 4E). We also examined the formation of local F-actin rich structures in flt-3 bone marrow-derived DCs treated with LPS to induce maturation. No compartment formation at sites of contact with the aggregate was observed in these mature flt-3 bone marrow-derived DCs (data not shown).

It has been shown that mDC contain higher basal levels of F-actin than iDC[47], which might partially account for the increased F-actin at sites of contact with agLDL. Thus, we next quantified another aspect of exophagy, the amount of lysosome exocytosis to the lysosomal synapse, in iDCs and mDCs. Biotin-fluorescein-dextran was delivered to DC lysosomes via overnight incubation[42]. Cells were then exposed to streptavidin-Alexa546-labeled agLDL for 90 min, and excess biotin was applied to block any remaining free streptavidin on the

aggregates. Cells were then fixed and permeabilized. Lysosome exocytosis was observed to aggregate-containing compartments in both iDCs (Figure 4F–H) and mDCs (Figure 4I–K). Again, mDCs exhibited a larger response to the aggregate as significantly more lysosome exocytosis to the lysosomal synapse was observed in mDCs than iDCs (Figure 4L). We also examined lysosome exocytosis in unsorted, $CD11c^+$ and $CD11c^-$ cells from the iDC culture. Consistent with previous results, no quantitative difference in lysosome exocytosis was seen between unsorted and $CD11c^+$ cells (Supplemental Figure IIB).

We confirmed that our DCs behaved as expected in regards to the activity of other maturation and endocytic mechanisms. Consistent with previous studies, major histocompatability complex II (MHC II) and CD86 were upregulated, and phagocytosis and macropinocytosis were down regulated upon DC maturation (Supplemental Figure III). Thus, despite the fact that macropinocytosis delivered significantly more biotin-fluorescein-dextran to the lysosomes of iDCs, less exocytosed fluorescein was detected during exophagy.

We also examined the amount of lysosome exocytosis in immature and mature huMDDCs and again found that mDCs exhibited more lysosome exocytosis to agLDL containing compartments than iDCs (Figure 4L). These data indicate a significant upregulation of exophagy, presumably indicative of greater agLDL catabolism, with DC maturation. Consistent with previous results, no lysosome exocytosis was observed in areas of contact with the aggregate in mature flt-3 bone marrow-derived DCs (data not shown).

We expected that greater actin polymerization and lysosome exocytosis might result in enhanced acidification of the lysosomal synapse in mDCs. We made live cell pH measurements of lysosomal synapses in iDCs and mDCs containing agLDL labeled with pH-sensitive and pH-insensitive fluorophores to determine the lowest pH achieved in the compartment following a 30 min agLDL incubation. We observed no significant differences in pH values obtained from lysosomal synapses in iDCs and mDCs (Figure 4M). Further, compartments used for exophagy by DCs were less acidic than those used by J774 macrophage-like cells (Figure 4M). This observation parallels previous work which found that DC phagosomes are less acidic than those of macrophages[48]. In spite of this, we did observe pH values in the lysosomal synapse as low as 5.5 in DCs (Figure 4M), indicating that sufficient acidification takes place to allow lysosomal enzymes, such as LAL, to be active[49].

AgLDL incubation causes mature GM-CSF bone marrow-derived DCs to accumulate more cellular free cholesterol than immature GM-CSF bone marrow-derived DCs

We examined the consequences of more robust lysosomal synapse formation on DC cholesterol internalization. Immature and mature non-classical DCs were incubated with agLDL for 0, 30 and 90 min in the presence of an ACAT inhibitor to prevent re-esterification of internalized cholesterol. At the indicated time points, cellular lipids were extracted, and amounts of free and total cholesterol were determined GC-MS. Following a 90 min incubation with agLDL, mDCs internalized more free cholesterol than iDCs (Figure 5). No significant difference was seen in the free cholesterol content of iDC and mDC after 30 min. These data are consistent with the results presented in Figure 4 indicating that

mDCs form larger F-actin dependent extracellular compartments and exhibit increased lysosome exocytosis to these compartments compared to iDCs. Taken together, these data suggest that exophagy is upregulated in mDCs compared to iDCs. This upregulation contrasts with various forms of endocytic internalization in DCs, such as macropinocytosis and phagocytosis, which are dampened with maturation[37, 38].

Monocyte-derived mature DCs isolated from murine atherosclerotic plaques accumulate more lipid than immature DCs

To examine the capacity of different DC subsets to accumulate lipid and form foam cells *in vivo*, we isolated DCs from the aorta of 5 ApoE−/− mice on a high fat diet for 12 weeks. Cell suspensions were prepared from the aortic root (valves and aortic sinus) and both ascending and descending aorta of the mice. The aorta was dissociated with an enzyme mixture and then stained with monoclonal antibodies, for dissecting DC subsets, and LipidTOX-Red, for quantifying neutral lipid content. The Steinman laboratory has previously used a similar approach to examine aortic leukocyte populations[11]. Although CD11c is commonly accepted as a pan-DC marker, a clear identification of DCs is still limited by the lack of unambiguous surface markers. In particular, the discrimination of DCs from macrophages that share many markers and functions remains challenging. Findings by the Steinman laboratory and others indicate that some macrophage foam cells can express CD11c[11, 50]. Thus, to avoid including macrophages in our analysis, cells that were $CD11b^{hi}$ were excluded from our analysis whether they were $CD11c^{+}$ or $CD11c^{-}$. However, we note that the CD11b expression is somewhat variable on both DCs and macrophages and perfect discrimination of these cell types is difficult.

Consistent with the studies of the Steinman laboratory, we observed a minor fraction of $CD11c^{+}$ and MHC II^{hi} cells in the aorta with low to intermediate levels of CD11b. These cells have previously been shown to possess immune-stimulating and cross-presentation capacities similar to DCs from lymphoid tissues[51]. $CD11c^{+}$ and MHC II^{hi} cells were further subdivided into mDCs and iDCs based on quantitative analysis of MHC II expression. Representative MHC $II^{hi}CD11c^{+}CD11b^{low}$, predominantly monocyte-derived mDC, and MHC $II^{int}CD11c^{+}CD11b^{low}$, predominantly monocyte-derived iDC are shown in Figure 6A–E. The mDC, highlighted with an arrow in Figure 6E, is positive for neutral lipid staining indicative of foam cell formation. A $CD11b^{hi}$ cell, possibly a macrophage, that was excluded from analysis can also be seen (Figure 6E).

We also examined the neutral lipid content of monocyte-independent DCs isolated from the plaque of ApoE−/− mice on a high fat diet for 12 weeks. Monocyte-independent DCs were defined by their expression of CD103, a ligand for E-cadherin expressed by most epithelial cells and also a marker for $CD11b^{-}$ DCs in many tissues[52–56]. Most $CD11b^{-}F4/80^{-}$ DCs express CD103 in normal murine aorta, and this molecule has not been found on any other population of aortic leukocytes[11]. Examples of $CD103^{+}Cd11c^{+}$ cells are shown in Figure 6F–I.

The LipidTOX signal per cell was quantified for each DC subset (Figure 6J). MHC $II^{hi}CD11c^{+}CD11b^{low}$ DCs contained more neutral lipid, indicative of foam cell formation, than MHC $II^{int}CD11c^{+}CD11b^{low}$ DCs. $CD103^{+}CD11c^{+}$ monocyte-independent DCs

contained scant amounts of neutral lipid compared to monocyte-derived DCs. These results demonstrate that our cell culture findings examining exophagy-mediated degradation of agLDL mirror *in vivo* patterns of DC subset neutral lipid accumulation.

Discussion

It has long been recognized that osteoclasts create extracellular lysosome-like compartments that play an essential role in bone remodeling[57, 58]. We have recently shown that a similar extracellular lysosomal hydrolysis process, termed exophagy, can be used by macrophages to clear large aggregates of LDL[36, 39]. Thus, we wondered whether DCs could also perform exophagy. Based on emerging evidence that DCs contribute to atherosclerotic foam cell formation, we investigated whether DCs, both flt-3 bone marrow-derived (monocyte-independent, classical) and GM-CSF bone marrow-derived (monocyte-derived, non-classical), could perform exophagy of aggregated lipoproteins.

Our studies elucidate the mechanism of a novel pathway for catabolism of agLDL by DCs and demonstrate that, in addition to macrophages and osteoclasts, monocyte-derived DCs are capable of exophagic degradation. When GM-CSF bone marrow-derived DCs were incubated with agLDL, the formation of extracellular aggregate-containing compartments was observed. Lysosomal contents were delivered to these compartments, and they were acidified, thereby enabling activation of lysosomal hydrolases. Together, these results demonstrate that during monocyte-derived DC engagement of agLDL, exophagic cholesteryl ester hydrolysis occurs as an initial step in foam cell formation. Conversely, flt-3 bone marrow-derived DCs did not exhibit exophagic degradation of agLDL and consequently, were unable to internalize the aggregate and did not become foam cells.

While revising our manuscript, heterogeneity in the GM-CSF mouse bone marrow culture system used in this study was reported [59]. Although this culture system has been widely used to generate $CD11c^{+}MHCII^{+}$ cells, previously considered a highly pure population of DCs, it was recently demonstrated that on day 6 of culture it is comprised of a small number of bona fide DCs, in addition to monocyte-derived macrophages and uncharacterized cells. These distinctions were made on the basis of ontogenetic, morphological and gene expression criteria. Culture conditions used to generate the mDC in this study were not examined using these criteria. While future studies will be needed to evaluate exophagy in the DC population defined in this manner, many of the cells in the current study exhibit morphological features, such as dendritic processes, characteristic of DCs (*e.g.* Figure 1A, Figure 2K and M), thus supporting the fact that monocyte-derived DCs can perform exophagy of agLDL.

We also investigated the efficiency of exophagy in iDC and mDC internalization of agLDL. In most tissues, DCs are present in an immature state. Forms of endocytosis, such as phagocytosis, macropinocytosis, and efferocytosis, are very efficient in iDCs and serve as a means of antigen capture[37, 38]. In response to inflammatory stimuli, DCs trigger the process of maturation, a terminal differentiation program required to initiate T-cell responses[60, 61]. Upon maturation, DCs exhibit reduced antigen capture capacity (down regulation of phagocytosis and macropinocytosis) and increased surface expression of MHC II and co-

stimulatory molecules[62, 63]. Thus, we were surprised to find that exophagy of agLDL was substantially more efficient in mDCs than iDCs. This finding may be particularly significant for atherogenesis as both human and animal studies have demonstrated the accumulation of mDC in atherosclerotic plaques with lesion progression[8]. Our results indicate that mDC will take up more lipid than iDC and will rapidly become foam cells. This may exacerbate plaque progression as DCs under conditions of hyperlipidemia exhibit a reduced migratory ability[29] and emigration with their lipid load may be impaired. However, the role of DC emigration during atherogenesis remains to be defined. Further, mDC are located mainly in rupture-prone areas of the plaque[8]. Thus, exophagy-mediated catabolism of agLDL by mDC may directly contribute to plaque instability through the release of lysosomal enzymes that could destabilize the collagen cap. Indeed, significantly higher numbers of DCs reside in carotid plaques with characteristics of vulnerable lesions than in stable lesions[8]. Thus, exophagic degradation of agLDL by DCs could play a role in plaque rupture and ensuing cardiac events.

Mature DCs serve two dominant functions; antigen presentation and migration to lymph nodes. It is possible that exophagy is increased in mDCs because it is related to the formation of the immunological synapse or, as has recently been suggested[64], is necessary for matrix degradation to facilitate cell migration. Alternatively, it has been shown that during maturation, DCs use tubular lysosomes to deliver MHCII to the plasma membrane[65]. Thus, it is possible that lysosome exocytosis occurs more readily in mDCs thereby enhancing exophagy. Our finding that exophagy is upregulated in mDC, taken together with recent data indicating that receptor-mediated endocytosis remains an efficient means of antigen internalization in mDC[66], indicate that the biology of DC maturation with regards to endocytosis is more complex than originally appreciated. Interestingly, several therapeutic interventions for atherosclerosis, such as aspirin and statins, have been shown to maintain DCs in an immature state[67, 68]. Our results suggest that in addition to quelling the inflammatory cascade associated with atherosclerosis, these therapies may also directly modulate the efficacy of DC foam cell formation.

Examination of foam cell formation in plaque DC subsets isolated from a standard mouse model of atherosclerosis showed that *in vivo* monocyte-derived mDCs (MHC $II^{hi}CD11c^{+}CD11b^{low}$ DCs) contain more neutral lipid than monocyte-derived iDCs (MHC $II^{int}CD11c^{+}CD11b^{low}$) while monocyte-independent DCs ($CD103^{+}CD11c^{+}$) contained scant amounts of lipid. These findings mirror our cell culture results. Based on our findings, we propose that rapid cholesteryl ester hydrolysis and the transfer of free cholesterol directly from LDL aggregates to non-classical DCs and macrophages may occur when these cells encounter subendothelial lipoproteins in developing atherosclerotic lesions. Further, the data expand the types of monocyte-derived cells known to perform exophagy.

Supplementary Material

Refer to Web version on PubMed Central for supplementary material.

Acknowledgments

Sources of Funding: This work was supported by National Institutes of Health grants R37-DK27083 and RO1-HL092234. R.K.S. is an American Heart Association Postdoctoral Fellow. H.F.C is a Merck Life Sciences Research Foundation Fellow.

Abbreviations List

ACAT	acyl-coenzyme A cholesterol acyltransferase
Alexa	AlexaFluor
agLDL	aggregated low density lipoprotein
CtB	cholera toxin subunit B
CypHer 5E	CypHer 5E Mono N-hydroxysuccinimide ester
DC	dendritic cell
flt-3	fms-like tyrosine kinase 3 ligand
GC-MS	gas chromatography-mass spectrometry
GM-CSF	granulocyte macrophage colony-stimulating factor
HEPES	4-(2-hydroxyethyl)-1-pipierazine ethane sulphonic acid
huMDDC	human monocyte derived dendritic cell
iDC	immature dendritic cell
LAL	lysosomal acid lipase
LDL	low density lipoprotein
LPS	lipopolysaccharide
mDC	mature dendritic cell
MHC II	major histocompatibility complex II
MβCD	methyl-β-cyclodextrin
RPMI	Roswell Park Memorial Institute

References

1. Bobryshev YV, Lord RS. Ultrastructural recognition of cells with dendritic cell morphology in human aortic intima. Contacting interactions of Vascular Dendritic Cells in athero-resistant and athero-prone areas of the normal aorta. Arch Histol Cytol. 1995; 58:307–322. [PubMed: 8527238]
2. Bobryshev YV, Lord RS. Structural heterogeneity and contacting interactions of vascular dendritic cells in early atherosclerotic lesions of the human aorta. J Submicrosc Cytol Pathol. 1996; 28:49–60. [PubMed: 8929626]
3. Bobryshev YV. Dendritic cells and their involvement in atherosclerosis. Current Opinion in Lipidology. 2000; 11:511–517. [PubMed: 11048894]
4. Bobryshev YV, Lord RS. S-100 positive cells in human arterial intima and in atherosclerotic lesions. Cardiovascular Research. 1995; 29:689–696. [PubMed: 7606759]

5. Bobryshev YV, Ikezawa T, Watanabe T. Formation of Birbeck granule-like structures in vascular dendritic cells in human atherosclerotic aorta. Lag-antibody to epidermal Langerhans cells recognizes cells in the aortic wall. Atherosclerosis. 1997; 133:193–202. [PubMed: 9298679]
6. Bobryshev YV, Lord RS. 55-kD actin-bundling protein (p55) is a specific marker for identifying vascular dendritic cells. J Histochem Cytochem. 1999; 47:1481–1486. [PubMed: 10544221]
7. Soilleux EJ, Morris LS, Trowsdale J, Coleman N, Boyle JJ. Human atherosclerotic plaques express DC-SIGN, a novel protein found on dendritic cells and macrophages. J Pathol. 2002; 198:511–516. [PubMed: 12434421]
8. Yilmaz A, Lochno M, Traeg F, Cicha I, Reiss C, Stumpf C, Raaz D, Anger T, Amann K, Probst T, Ludwig J, Daniel WG, Garlichs CD. Emergence of dendritic cells in rupture-prone regions of vulnerable carotid plaques. Atherosclerosis. 2004; 176:101–110. [PubMed: 15306181]
9. Erbel C, Sato K, Meyer FB, Kopecky SL, Frye RL, Goronzy JJ, Weyand CM. Functional profile of activated dendritic cells in unstable atherosclerotic plaque. Basic Res Cardiol. 2007; 102:123–132. [PubMed: 17136419]
10. Zernecke A. Dendritic Cells in Atherosclerosis: Evidence in Mice and Humans. Arteriosclerosis, Thrombosis & Vascular Biology. 2015
11. Choi JH, Cheong C, Dandamudi DB, Park CG, Rodriguez A, Mehandru S, Velinzon K, Jung IH, Yoo JY, Oh GT, Steinman RM. Flt3 signaling-dependent dendritic cells protect against atherosclerosis. Immunity. 2011; 35:819–831. [PubMed: 22078798]
12. Butcher MJ, Galkina EV. Phenotypic and functional heterogeneity of macrophages and dendritic cell subsets in the healthy and atherosclerosis-prone aorta. Front Physiol. 2012; 3:44. [PubMed: 22457649]
13. Subramanian M, Tabas I. Dendritic cells in atherosclerosis. Semin Immunopathol. 2014; 36:93–102. [PubMed: 24196454]
14. Randolph GJ. Mechanisms that regulate macrophage burden in atherosclerosis. Circulation Research. 2014; 114:1757–1771. [PubMed: 24855200]
15. Koltsova EK, Garcia Z, Chodaczek G, Landau M, McArdle S, Scott SR, von Vietinghoff S, Galkina E, Miller YI, Acton ST, Ley K. Dynamic T cell-APC interactions sustain chronic inflammation in atherosclerosis. Journal of Clinical Investigation. 2012; 122:3114–3126. [PubMed: 22886300]
16. Chistiakov DA, Sobenin IA, Orekhov AN, Bobryshev YV. Dendritic cells in atherosclerotic inflammation: the complexity of functions and the peculiarities of pathophysiological effects. Front Physiol. 2014; 5:196. [PubMed: 24904430]
17. Gautier EL, Huby T, Saint-Charles F, Ouzilleau B, Pirault J, Deswaerte V, Ginhoux F, Miller ER, Witztum JL, Chapman MJ, Lesnik P. Conventional dendritic cells at the crossroads between immunity and cholesterol homeostasis in atherosclerosis. Circulation. 2009; 119:2367–2375. [PubMed: 19380622]
18. Paulson KE, Zhu SN, Chen M, Nurmohamed S, Jongstra-Bilen J, Cybulsky MI. Resident intimal dendritic cells accumulate lipid and contribute to the initiation of atherosclerosis. Circulation Research. 2010; 106:383–390. [PubMed: 19893012]
19. Naik SH, Metcalf D, van Nieuwenhuijze A, Wicks I, Wu L, O'Keeffe M, Shortman K. Intrasplenic steady-state dendritic cell precursors that are distinct from monocytes. Nature Immunology. 2006; 7:663–671. [PubMed: 16680143]
20. Onai N, Obata-Onai A, Tussiwand R, Lanzavecchia A, Manz MG. Activation of the Flt3 signal transduction cascade rescues and enhances type I interferon-producing and dendritic cell development. Journal of Experimental Medicine. 2006; 203:227–238. [PubMed: 16418395]
21. Liu K, Victora GD, Schwickert TA, Guermonprez P, Meredith MM, Yao K, Chu FF, Randolph GJ, Rudensky AY, Nussenzweig M. In vivo analysis of dendritic cell development and homeostasis. Science. 2009; 324:392–397. [PubMed: 19286519]
22. Cheong C, Matos I, Choi JH, Dandamudi DB, Shrestha E, Longhi MP, Jeffrey KL, Anthony RM, Kluger C, Nchinda G, Koh H, Rodriguez A, Idoyaga J, Pack M, Velinzon K, Park CG, Steinman RM. Microbial stimulation fully differentiates monocytes to DC-SIGN/CD209(+) dendritic cells for immune T cell areas. Cell. 2010; 143:416–429. [PubMed: 21029863]

23. Liu P, Yu YR, Spencer JA, Johnson AE, Vallanat CT, Fong AM, Patterson C, Patel DD. CX3CR1 deficiency impairs dendritic cell accumulation in arterial intima and reduces atherosclerotic burden. Arteriosclerosis, Thrombosis & Vascular Biology. 2008; 28:243–250.
24. Ditiatkovski M, Toh BH, Bobik A. GM-CSF deficiency reduces macrophage PPAR-gamma expression and aggravates atherosclerosis in ApoE-deficient mice. Arteriosclerosis, Thrombosis & Vascular Biology. 2006; 26:2337–2344.
25. Shaposhnik Z, Wang X, Weinstein M, Bennett BJ, Lusis AJ. Granulocyte macrophage colony-stimulating factor regulates dendritic cell content of atherosclerotic lesions. Arteriosclerosis, Thrombosis & Vascular Biology. 2007; 27:621–627.
26. Combadiere C, Potteaux S, Gao JL, Esposito B, Casanova S, Lee EJ, Debre P, Tedgui A, Murphy PM, Mallat Z. Decreased atherosclerotic lesion formation in CX3CR1/apolipoprotein E double knockout mice. Circulation. 2003; 107:1009–1016. [PubMed: 12600915]
27. Moore KJ, Tabas I. Macrophages in the pathogenesis of atherosclerosis. Cell. 2011; 145:341–355. [PubMed: 21529710]
28. Jakubzick C, Tacke F, Llodra J, van Rooijen N, Randolph GJ. Modulation of dendritic cell trafficking to and from the airways. Journal of Immunology. 2006; 176:3578–3584.
29. Angeli V, Llodra J, Rong JX, Satoh K, Ishii S, Shimizu T, Fisher EA, Randolph GJ. Dyslipidemia associated with atherosclerotic disease systemically alters dendritic cell mobilization. Immunity. 2004; 21:561–574. [PubMed: 15485633]
30. Boren J, Gustafsson M, Skalen K, Flood C, Innerarity TL. Role of extracellular retention of low density lipoproteins in atherosclerosis. Curr Opin Lipidol. 2000; 11:451–456. [PubMed: 11048887]
31. Tabas I. Nonoxidative modifications of lipoproteins in atherogenesis. Annu Rev Nutr. 1999; 19:123–139. [PubMed: 10448519]
32. Smith EB, Massie IB, Alexander KM. The release of an immobilized lipoprotein fraction from atherosclerotic lesions by incubation with plasmin. Atherosclerosis. 1976; 25:71–84. [PubMed: 186079]
33. Skalen K, Gustafsson M, Rydberg EK, Hulten LM, Wiklund O, Innerarity TL, Boren J. Subendothelial retention of atherogenic lipoproteins in early atherosclerosis. Nature. 2002; 417:750–754. [PubMed: 12066187]
34. Brown MS, Goldstein JL, Krieger M, Ho YK, Anderson RG. Reversible accumulation of cholesteryl esters in macrophages incubated with acetylated lipoproteins. Journal of Cell Biology. 1979; 82:597–613. [PubMed: 229107]
35. Goldstein JL, Ho YK, Basu SK, Brown MS. Binding site on macrophages that mediates uptake and degradation of acetylated low density lipoprotein, producing massive cholesterol deposition. Proceedings of the National Academy of Sciences of the United States of America. 1979; 76:333–337. [PubMed: 218198]
36. Haka AS, Grosheva I, Chiang E, Buxbaum AR, Baird BA, Pierini LM, Maxfield FR. Macrophages create an acidic extracellular hydrolytic compartment to digest aggregated lipoproteins. Molecular Biology of the Cell. 2009; 20:4932–4940. [PubMed: 19812252]
37. Sallusto F, Cella M, Danieli C, Lanzavecchia A. Dendritic cells use macropinocytosis and the mannose receptor to concentrate macromolecules in the major histocompatibility complex class II compartment: downregulation by cytokines and bacterial products. Journal of Experimental Medicine. 1995; 182:389–400. [PubMed: 7629501]
38. Garrett WS, Chen LM, Kroschewski R, Ebersold M, Turley S, Trombetta S, Galan JE, Mellman I. Developmental control of endocytosis in dendritic cells by Cdc42. Cell. 2000; 102:325–334. [PubMed: 10975523]
39. Grosheva I, Haka AS, Qin C, Pierini LM, Maxfield FR. Aggregated LDL in contact with macrophages induces local increases in free cholesterol levels that regulate local actin polymerization. Arteriosclerosis, Thrombosis & Vascular Biology. 2009; 29:1615–1621.
40. Mayor S, Rothberg KG, Maxfield FR. Sequestration of GPI-anchored proteins in caveolae triggered by cross-linking. Science. 1994; 264:1948–1951. [PubMed: 7516582]
41. Naik SH, Proietto AI, Wilson NS, Dakic A, Schnorrer P, Fuchsberger M, Lahoud MH, O'Keeffe M, Shao QX, Chen WF, Villadangos JA, Shortman K, Wu L. Cutting edge: generation of splenic

CD8+ and CD8− dendritic cell equivalents in Fms-like tyrosine kinase 3 ligand bone marrow cultures. Journal of Immunology. 2005; 174:6592–6597.

42. Mukherjee S, Ghosh RN, Maxfield FR. Endocytosis. Physiological Reviews. 1997; 77:759–803. [PubMed: 9234965]
43. Buton X, Mamdouh Z, Ghosh R, Du H, Kuriakose G, Beatini N, Grabowski GA, Maxfield FR, Tabas I. Unique cellular events occurring during the initial interaction of macrophages with matrix-retained or methylated aggregated low density lipoprotein (LDL). Prolonged cell-surface contact during which ldl-cholesteryl ester hydrolysis exceeds ldl protein degradation. Journal of Biological Chemistry. 1999; 274:32112–32121. [PubMed: 10542246]
44. Beletskii A, Cooper M, Sriraman P, Chiriac C, Zhao L, Abbot S, Yu L. High-throughput phagocytosis assay utilizing a pH-sensitive fluorescent dye. Biotechniques. 2005; 39:894–897. [PubMed: 16382909]
45. Qin C, Nagao T, Grosheva I, Maxfield FR, Pierini LM. Elevated plasma membrane cholesterol content alters macrophage signaling and function. Arteriosclerosis, Thrombosis & Vascular Biology. 2006; 26:372–378.
46. Inaba K, Swiggard WJ, Steinman RM, Romani N, Schuler G, Brinster C. Isolation of dendritic cells. Curr Protoc Immunol. 2009; Chapter 3(Unit 3):7. [PubMed: 19653207]
47. Verdijk P, van Veelen PA, de Ru AH, Hensbergen PJ, Mizuno K, Koerten HK, Koning F, Tensen CP, Mommaas AM. Morphological changes during dendritic cell maturation correlate with cofilin activation and translocation to the cell membrane. Eur J Immunol. 2004; 34:156–164. [PubMed: 14971041]
48. Savina A, Jancic C, Hugues S, Guermonprez P, Vargas P, Moura IC, Lennon-Dumenil AM, Seabra MC, Raposo G, Amigorena S. NOX2 controls phagosomal pH to regulate antigen processing during crosspresentation by dendritic cells. Cell. 2006; 126:205–218. [PubMed: 16839887]
49. Sheriff S, Du H, Grabowski GA. Characterization of lysosomal acid lipase by site-directed mutagenesis and heterologous expression. Journal of Biological Chemistry. 1995; 270:27766–27772. [PubMed: 7499245]
50. Cho HJ, Shashkin P, Gleissner CA, Dunson D, Jain N, Lee JK, Miller Y, Ley K. Induction of dendritic cell-like phenotype in macrophages during foam cell formation. Physiol Genomics. 2007; 29:149–160. [PubMed: 17244792]
51. Choi JH, Do Y, Cheong C, Koh H, Boscardin SB, Oh YS, Bozzacco L, Trumpfheller C, Park CG, Steinman RM. Identification of antigen-presenting dendritic cells in mouse aorta and cardiac valves. Journal of Experimental Medicine. 2009; 206:497–505. [PubMed: 19221394]
52. Annacker O, Coombes JL, Malmstrom V, Uhlig HH, Bourne T, Johansson-Lindbom B, Agace WW, Parker CM, Powrie F. Essential role for CD103 in the T cell-mediated regulation of experimental colitis. Journal of Experimental Medicine. 2005; 202:1051–1061. [PubMed: 16216886]
53. Edelson BT, Kc W, Juang R, Kohyama M, Benoit LA, Klekotka PA, Moon C, Albring JC, Ise W, Michael DG, Bhattacharya D, Stappenbeck TS, Holtzman MJ, Sung SS, Murphy TL, Hildner K, Murphy KM. Peripheral CD103+ dendritic cells form a unified subset developmentally related to CD8alpha+ conventional dendritic cells. Journal of Experimental Medicine. 2010; 207:823–836. [PubMed: 20351058]
54. Johansson-Lindbom B, Svensson M, Pabst O, Palmqvist C, Marquez G, Forster R, Agace WW. Functional specialization of gut CD103+ dendritic cells in the regulation of tissue-selective T cell homing. Journal of Experimental Medicine. 2005; 202:1063–1073. [PubMed: 16216890]
55. Merad M, Manz MG. Dendritic cell homeostasis. Blood. 2009; 113:3418–3427. [PubMed: 19176316]
56. Sung SS, Fu SM, Rose CE Jr, Gaskin F, Ju ST, Beaty SR. A major lung CD103 (alphaE)-beta7 integrin-positive epithelial dendritic cell population expressing Langerin and tight junction proteins. Journal of Immunology. 2006; 176:2161–2172.
57. Jurdic P, Saltel F, Chabadel A, Destaing O. Podosome and sealing zone: specificity of the osteoclast model. Eur J Cell Biol. 2006; 85:195–202. [PubMed: 16546562]
58. Stenbeck G. Formation and function of the ruffled border in osteoclasts. Semin Cell Dev Biol. 2002; 13:285–292. [PubMed: 12243728]

59. Helft J, Bottcher J, Chakravarty P, Zelenay S, Huotari J, Schraml BU, Goubau D, Reis ESC. GM-CSF Mouse Bone Marrow Cultures Comprise a Heterogeneous Population of CD11c(+)MHCII(+) Macrophages and Dendritic Cells. Immunity. 2015; 42:1197–1211. [PubMed: 26084029]

60. Mellman I, Steinman RM. Dendritic cells: specialized and regulated antigen processing machines. Cell. 2001; 106:255–258. [PubMed: 11509172]

61. Trombetta ES, Mellman I. Cell biology of antigen processing in vitro and in vivo. Annu Rev Immunol. 2005; 23:975–1028. [PubMed: 15771591]

62. Pierre P, Turley SJ, Gatti E, Hull M, Meltzer J, Mirza A, Inaba K, Steinman RM, Mellman I. Developmental regulation of MHC class II transport in mouse dendritic cells. Nature. 1997; 388:787–792. [PubMed: 9285592]

63. Palm NW, Medzhitov R. Pattern recognition receptors and control of adaptive immunity. Immunol Rev. 2009; 227:221–233. [PubMed: 19120487]

64. Puissant E, Gilis F, Dogne S, Flamion B, Jadot M, Boonen M. Subcellular trafficking and activity of Hyal-1 and its processed forms in murine macrophages. Traffic. 2014; 15:500–515. [PubMed: 24502338]

65. Chow A, Toomre D, Garrett W, Mellman I. Dendritic cell maturation triggers retrograde MHC class II transport from lysosomes to the plasma membrane. Nature. 2002; 418:988–994. [PubMed: 12198549]

66. Platt CD, Ma JK, Chalouni C, Ebersold M, Bou-Reslan H, Carano RA, Mellman I, Delamarre L. Mature dendritic cells use endocytic receptors to capture and present antigens. Proceedings of the National Academy of Sciences of the United States of America. 2010; 107:4287–4292. [PubMed: 20142498]

67. Hackstein H, Morelli AE, Larregina AT, Ganster RW, Papworth GD, Logar AJ, Watkins SC, Falo LD, Thomson AW. Aspirin inhibits in vitro maturation and in vivo immunostimulatory function of murine myeloid dendritic cells. Journal of Immunology. 2001; 166:7053–7062.

68. Yilmaz A, Reiss C, Weng A, Cicha I, Stumpf C, Steinkasserer A, Daniel WG, Garlichs CD. Differential effects of statins on relevant functions of human monocyte-derived dendritic cells. Journal of Leukocyte Biology. 2006; 79:529–538. [PubMed: 16387846]

Significance

We show that monocyte-derived dendritic cells can degrade aggregated LDL (the predominant form of LDL found in atherosclerotic plaques), while monocyte-independent dendritic cells cannot. Monocyte-derived dendritic cells use a specialized form of catabolism to clear the LDL aggregates in which the cells create an extracellular, acidic compartment into which they secrete lysosomal enzymes. The interaction results in foam cell formation and, surprisingly, is upregulated upon dendritic cell maturation. This contrasts with various forms of endocytic internalization in dendritic cells, which decrease upon maturation. This finding may be significant for atherogenesis as studies have shown accumulation of mature dendritic cells in rupture-prone areas of the plaque. Thus, extracellular catabolism of aggregated LDL by mature dendritic cells may contribute to plaque instability through the release of lysosomal enzymes that could destabilize the collagen cap.

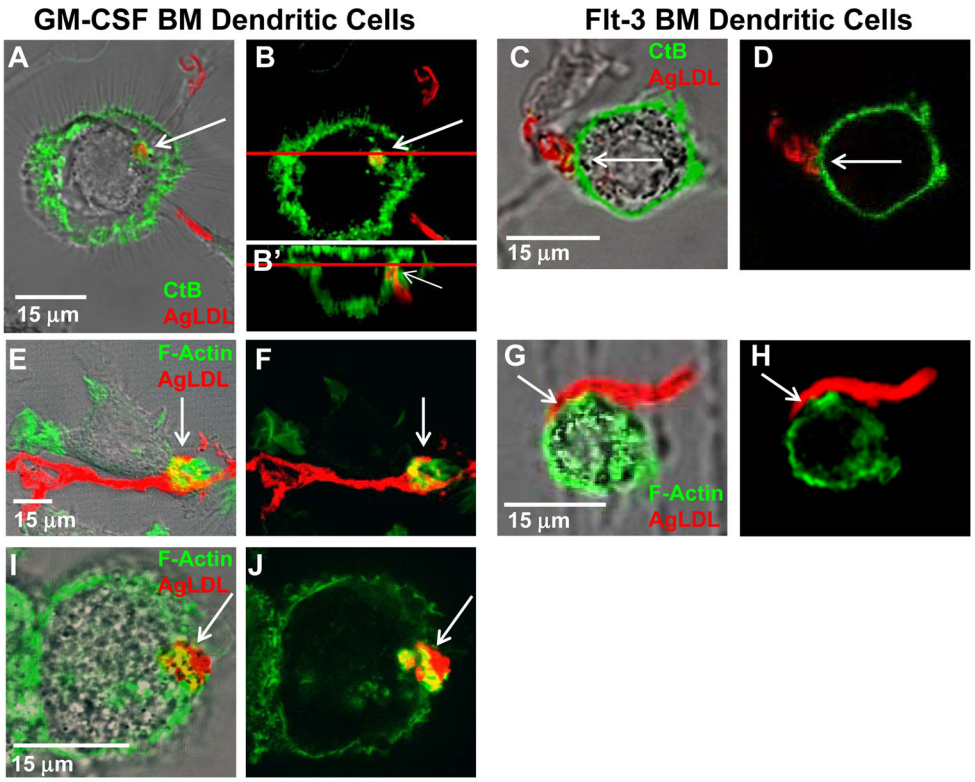

Figure 1. GM-CSF bone marrow-derived DCs form extracellular compartments at sites of contact with agLDL but flt-3 bone marrow-derived DCs do not

(A–J) GM-CSF BM (A, B and E, F and I, J) and flt-3 BM (C, D and G, H) DCs were incubated with Alexa546-agLDL (red) for 60 min and the interface between the aggregate and cells examined. (A–D) The plasma membrane was labeled via incubation with Alexa488-CtB (green) on ice for 3 min. Cells were than washed and fixed. Sites of contact between mature GM-CSF BM DCs and agLDL were labeled by CtB (arrows, A and B). An axial slice through the confocal stack at the position of the red line shows that, although the aggregate resembles a separate vesicle in the xy plane (B), it is contained in a compartment contiguous with the extracellular space (arrow, B′). Flt-3 BM DCs do not surround the aggregate with CtB positive membrane at sites of contact (arrows, C and D). (E–J) Cells were stained with Alexa488-phalloidin to show F-actin (green). An enrichment of F-actin was detected near the sites of contact with agLDL in GM-CSF BM (arrows, E and F) but not flt-3 BM (arrows, G and H) DCs. (I and J) Actin polymerization, at sites of contact with agLDL was also seen in mature huMDDCs (arrows, I and J).

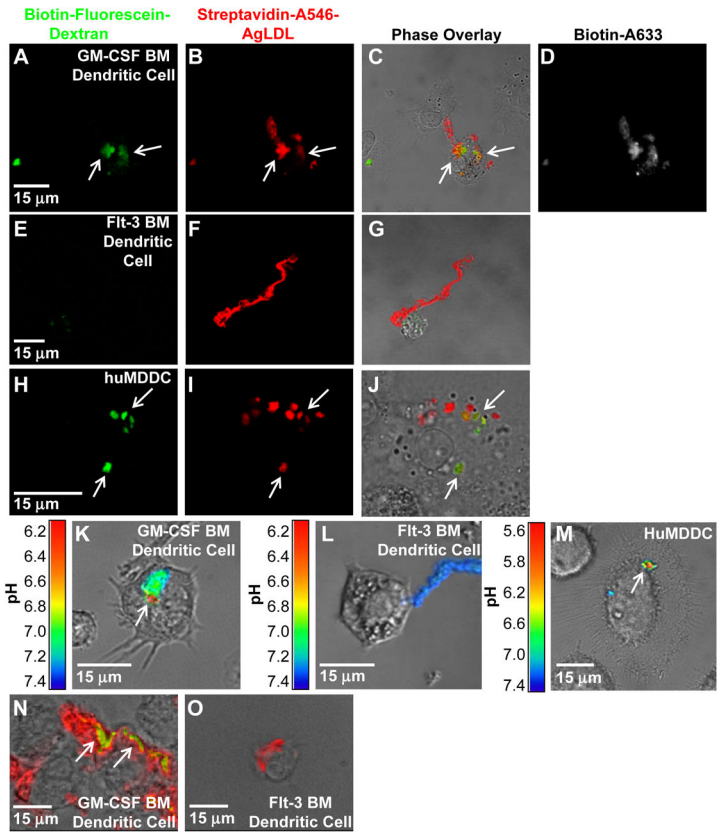

Figure 2. GM-CSF BM DCs use exophagy to degrade agLDL but flt-3 BM DCs do not

(A–J) GM-CSF BM and flt-3 BM DC lysosomes were loaded with biotin-fluorescein-dextran via overnight incubation. DCs were subsequently incubated with streptavidin and Alexa546 dual-labeled agLDL for 90 min, fixed and permeabilized. Colocalization of dextran (green) with the aggregate (red) indicates areas of exocytosis in mature GM-CSF BM DCs (arrows, A–C). A short pulse of Alexa633-biotin prior to fixation confirmed that the agLDL was still contained in an extracellular compartment (D). No lysosome exocytosis to areas of contact with the aggregate was observed in flt-3 BM DCs (E–G). Lysosome exocytosis to an extracellular agLDL containing compartment was confirmed in mature huMDDCs (arrows, H–J). (K–M) GM-CSF BM and flt-3 BM DCs were incubated with CypHer 5E, a pH sensitive fluorophore, and Alexa488, a pH insensitive fluorophore, dual-labeled agLDL and the pH surrounding the aggregate was measured. When mature GM-CSF BM DCs interacted with the dual-labeled agLDL, regions of low pH could be seen at the contact sites (K). No acidification was observed in aggregates in contact with classical DCs (L). Regions of low pH were also seen in contact sites between mature huMDDCs and agLDL (M). (N and O) GM-CSF BM and flt-3 BM DCs were incubated with Alexa546-agLDL for 1 hr, fixed and stained with filipin to indicate free cholesterol. (N) Cholesterol accumulation can be seen in compartments containing agLDL in an immature GM-CSF BM DC (arrows). (O) No cholesterol generation was observed when flt-3 BM DCs were incubated with agLDL.

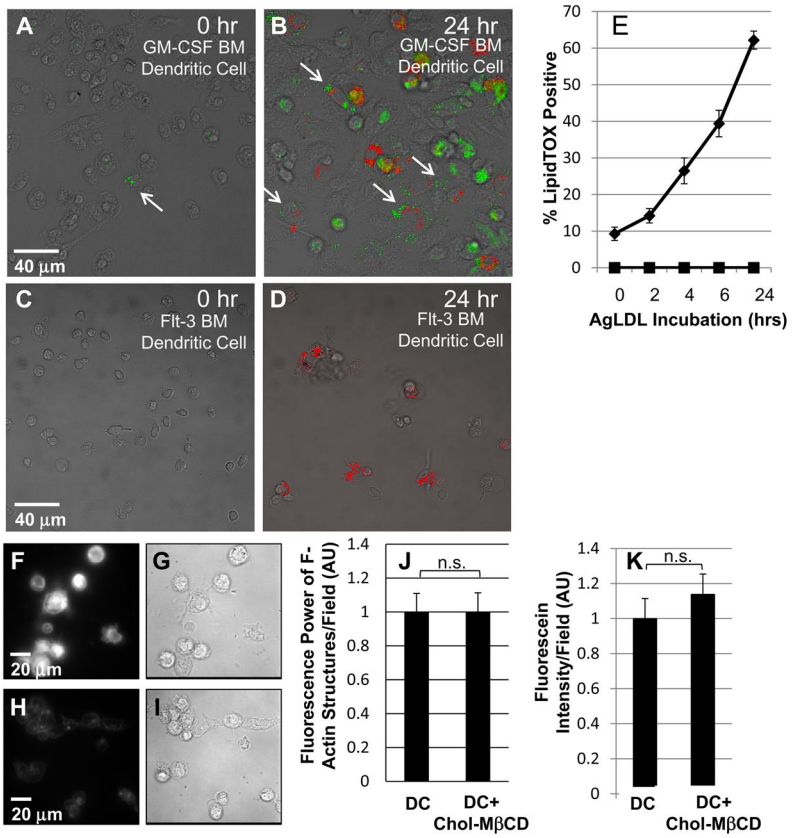

Figure 3. GM-CSF BM DCs incubated with agLDL form foam cells but flt-3 BM DCs do not

Immature GM-CSF BM DCs and flt-3 BM DCs were incubated with Alexa546-agLDL (red) for 0, 2, 4, 6 and 24 hrs. Cells were then fixed and stained with LipidTOX (green) to assess neutral lipid droplet formation. (A) Few LipidTOX positive non-classical DCs (arrow) are seen in the absence of agLDL. (B) GM-CSF BM DCs incubated with Alexa546-agLDL for 24 hrs form foam cells. Arrows indicate DCs in contact with agLDL containing LipidTOX positive droplets. (C) No LipidTOX positive flt-3 BM DCs are seen in the absence of agLDL. (D) Flt-3 BM DCs incubated with Alexa546-agLDL for 24hrs are negative for LipidTOX staining and do not form foam cells. (E) Quantification of the number of cells containing LipidTOX positive droplets as a function of agLDL incubation time. Diamonds: GM-CSF BM DCs, squares: flt-3 BM DCs. Error bars represent the standard error of the mean (sem). Data are pooled from 3 independent experiments for GM-CSF BM DCs and 2 independent experiments for flt-3 BM DCs. (F and G) Filipin and DIC image of immature GM-CSF BM DCs treated with 5mM cholesterol-MβCD for 15 min. (H and I) Filipin and DIC image of resting immature GM-CSF BM DCs. (J) Cholesterol loaded and resting immature GM-CSF BM DCs were incubated with Alexa546-agLDL for 60 min in the presence of an ACAT inhibitor followed by fixation, labeling of F-actin with Alexa488-phalloidin and quantification of the average local F-actin intensity per cell. (K) Cholesterol loaded and resting immature GM-CSF BM DCs with lysosomes labeled with biotin-fluorescein-dextran were incubated with streptavidin-Alexa546-labeled agLDL for 90 min in the presence of an ACAT inhibitor, fixed and permeabilized. The amount of biotin-

fluorescein-dextran exocytosed was quantified. Data are pooled from 2 independent experiments. Student’s t test n.s. not significant.

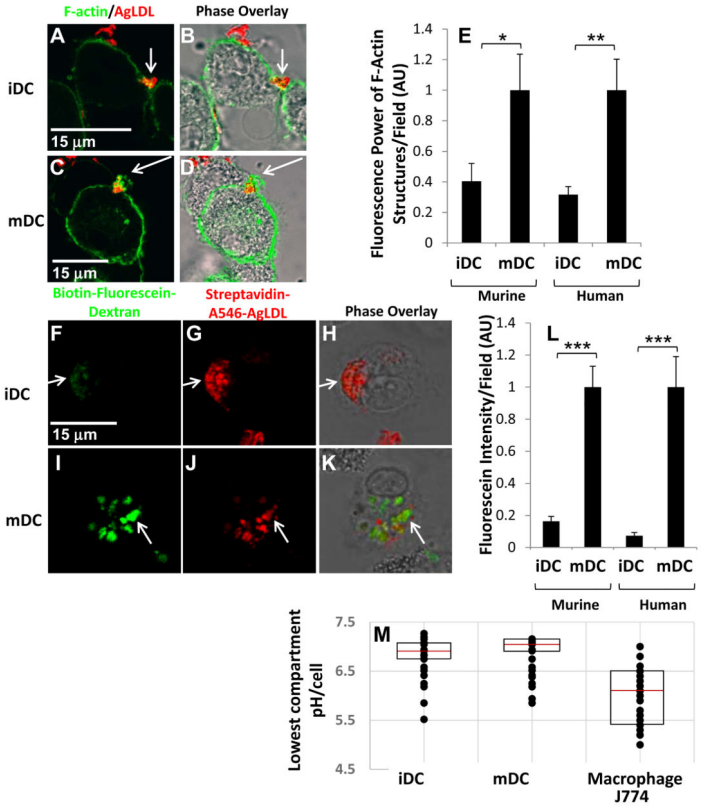

Figure 4. Exophagy is upregulated with DC maturation

(A–D) GM-CSF BM iDCs and mDCs were incubated with Alexa546-agLDL for 60 min followed by fixation and labeling of F-actin with Alexa488-phalloidin. After 60 min, an enrichment of F-actin was detected near the sites of contact with agLDL in both GM-CSF BM iDCs (A and B) and mDCs (C and D). (E) Quantification of the average local F-actin intensity per cell in both murine and human monocyte derived iDCs and mDCs. (F–H) GM-CSF BM iDCs and mDCs were incubated with biotin-fluorescein-dextran overnight to deliver it to lysosomes. Cells were then exposed to streptavidin-Alexa546-labeled agLDL for 90 min, fixed and permeabilized. Lysosome exocytosis was observed to aggregate containing compartments in both GM-CSF BM iDCs (F–H) and mDCs (I–K). (L) Quantification of the amount of biotin-fluorescein-dextran exocytosed in both murine and human monocyte derived iDC and mDC. (M) GM-CSF BM iDCs, mDCs and J774 macrophage-like cells were incubated with CypHer 5E, a pH sensitive fluorophore, and Alexa488, a pH insensitive fluorophore, dual-labeled agLDL and the pH surrounding the aggregate measured. Quantification of the lowest pH achieved in the compartment at a single timepoint in iDCs, mDCs and J774 macrophage-like cells. The central mark on each box is the median, while the edges of the box represent the 25th and 75th percentiles. Error bars (E and L) represent the sem. * $p \leq 0.05$, ** $p \leq 0.01$, *** $p \leq 0.001$ student's t test. Data are pooled from 3 independent experiments.

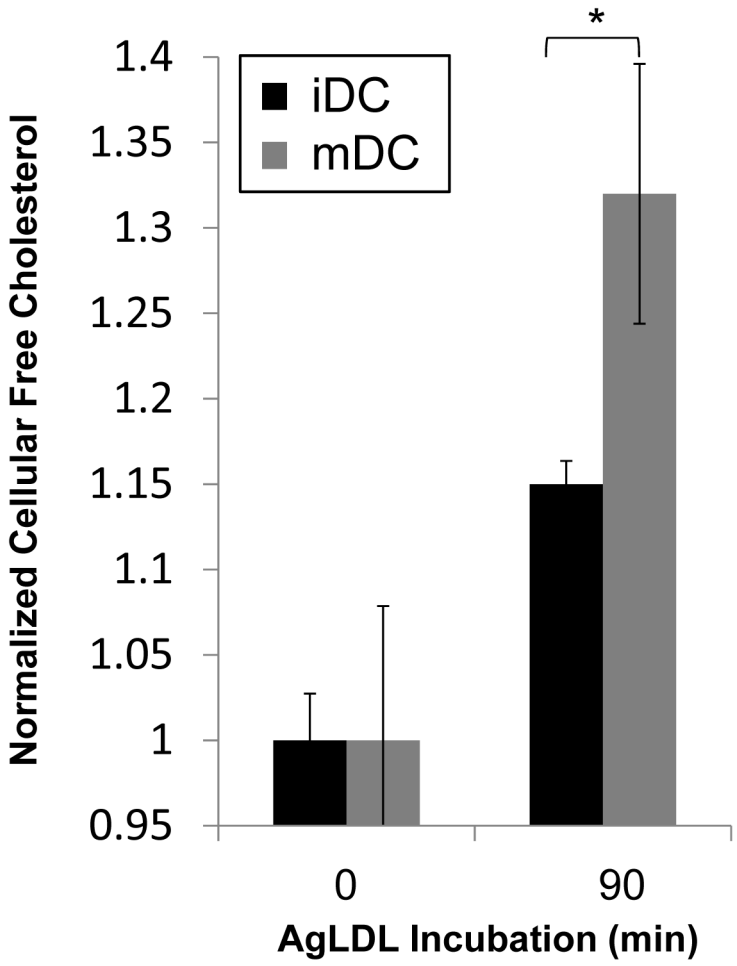

Figure 5. Mature DC accumulate more free cholesterol than immature DC upon incubation with agLDL

Immature and mature DCs were incubated with agLDL for 0, 30 or 90 min. Lipids were extracted and free cholesterol determined by GC-MS analysis. Values were normalized for extraction using β-sitosterol and for protein content. No significant difference was seen in the free cholesterol content of iDC and mDC at 30 min (data not shown). Error bars represent the sem. * $p \leq 0.05$ student's t test. Data pooled from 3 independent experiments.

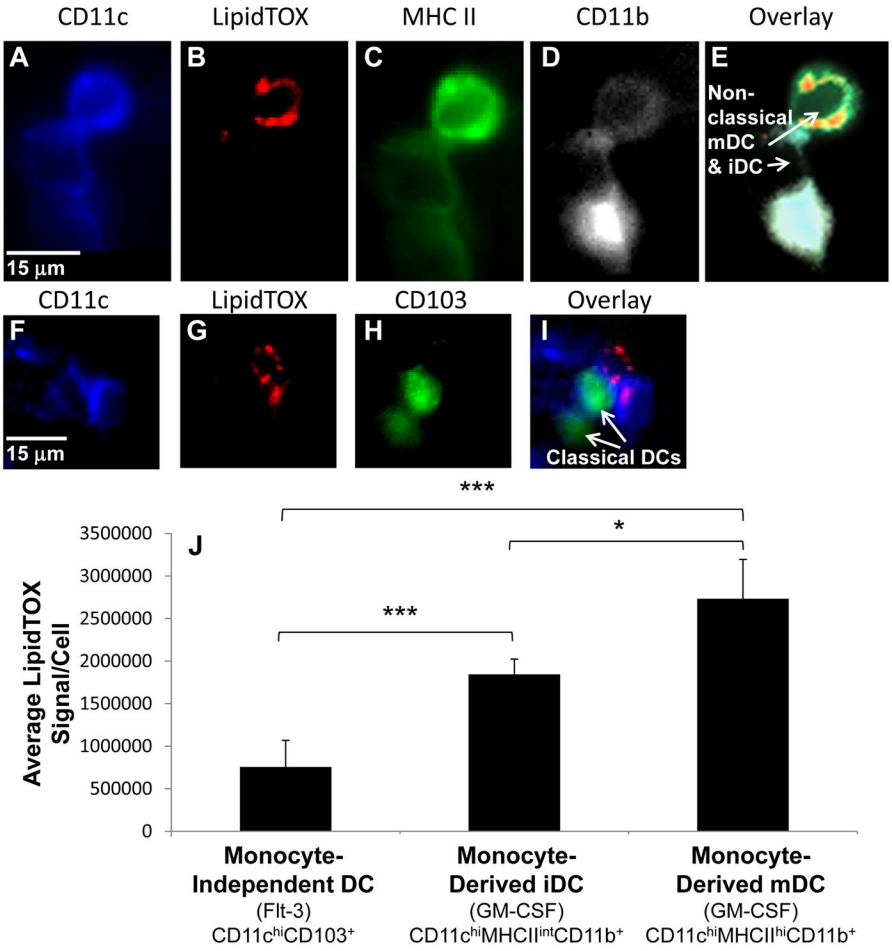

Figure 6. Lipid accumulation in DCs isolated from murine atherosclerotic plaques parallels *in vitro* results

Cells present in atherosclerotic plaques of 5 ApoE−/− mice on a high fat diet for 12 weeks were isolated and stained with monoclonal antibodies, for dissecting DC subsets, and LipidTOX-Red, for quantifying neutral lipid content. Quantitative analysis was used to delineate DC subsets. (A–E) Examples of a $CD11c^{hi}MHCII^{int}CD11b^{+}$ moncyte-derived iDC and a $CD11c^{hi}MHCII^{hi}CD11b^{+}$ monocyte-derived mDC (arrows, E). Cells with high CD11b expression were excluded from analysis. (F–I) Examples of $CD103^{+}CD11c^{+}$ monocyte-independent DCs (arrows, I). (J) Quantification of the LipidTOX signal per cell for each DC subset. Error bars represent the sem. * $p \leq 0.05$, *** $p \leq 0.001$ Kruskal-Wallis test followed by Wilcoxon rank-sum test.